

Bayesian Inference of the Evolution of a Phenotype Distribution on a Phylogenetic Tree

M. Azim Ansari¹ and Xavier Didelot^{2,*}

1 Oxford Martin School, University of Oxford, Oxford, OX1 3BD, United Kingdom

2 Department of Infectious Disease Epidemiology, Imperial College London, Norfolk Place, London, W2 1PG, United Kingdom

* Corresponding author: `x.didelot@imperial.ac.uk`

Abstract

The distribution of a phenotype on a phylogenetic tree is often a quantity of interest. Many phenotypes have imperfect heritability, so that a measurement of the phenotype for an individual can be thought of as a single realisation from the phenotype distribution of that individual. If all individuals in a phylogeny had the same phenotype distribution, measured phenotypes would be randomly distributed on the tree leaves. This is however often not the case, implying that the phenotype distribution evolves over time. Here we propose a new model based on this principle of evolving phenotype distribution on the branches of a phylogeny, which is different from ancestral state reconstruction where the phenotype itself is assumed to evolve. We develop an efficient Bayesian inference method to estimate the parameters of our model and to test the evidence for changes in the phenotype distribution. We use multiple simulated datasets to show that our algorithm has good sensitivity and specificity properties. Since our method identifies branches on the tree on which the phenotype distribution has changed, it is able to break down a tree into components for which this distribution is unique and constant. We present two applications of our method, one investigating the association between HIV genetic variation and human leukocyte antigen, and the other studying host range distribution in a lineage of *Salmonella enterica*, and we discuss many other potential applications. All the methods described in this paper are implemented in a software package called TreeBreaker which is freely available for download at <https://github.com/ansariazim/TreeBreaker>

Introduction

21

Understanding phenotypic variations and their relative association with genotypic variations is one of the central aims of molecular biology. The expression of a phenotype is usually dependent on both genetic and environmental factors, with heritability measuring their relative importance [1]. When the heritability is non-zero, genetically similar individuals are more likely to have similar phenotypes, and this is especially relevant for species that reproduce clonally, so that closely related individuals are virtually identical genetically. However, genotype-phenotype maps are usually complex and phenotypic plasticity means that phenotype expression can differ even for genetically identical individuals due to dependency on environmental factors [2, 3]. Conversely, observing closely related individuals with the same phenotype does not necessarily imply a low importance of environmental factors, since close relatives are also likely to live in the same environmental conditions [1]. The same effect also occurs in sexually reproducing species as evolutionary forces such as spatial population structure, environmental pressures and inbreeding result in groups within which individuals are more genetically homologous, and therefore more phenotypically similar, than individuals from different groups [4, 5].

To understand the relationship between a phenotype and a genotype, it is necessary to investigate how the phenotype is distributed according to genotypic values. This requires to quantify how the genotypes are related to each other which is often achieved using phylogenetic trees [6]. For clonal organisms, the tree may represent the clonal genealogy of how individuals are related with one another for non-recombinant regions [7, 8]. For sexual organisms, the phylogenies may be built for individual genomic loci, resulting in so-called gene trees by contrast with the species tree which contains them [9]. Visual inspection of a phylogenetic tree with tips annotated by phenotypes gives a first impression of their

relationship, and this type of figure features heavily in the molecular biology literature of both clonal and sexual organisms. A more quantitative approach is however needed if the tree is too large to be shown, the interesting patterns too subtle to be seen, or to estimate evolutionary parameters and test competing hypotheses.

Phylogenetic comparative methods can be used, for example to test the phylogenetic signal in a phenotype [10, 11] or to compare the association between two phenotypes given the phylogeny [12], but do not provide a complete description of the phenotype distribution on a tree. Ancestral state reconstruction of the phenotype given the tree [13, 14] is often used for this and can provide quantitative insights, for example an estimate of the phenotypic evolutionary rate. The maximum likelihood approach to ancestral state reconstruction [15] has been extended in many ways by refining the model of phenotypic evolution on the tree, for example allowing to detect branches where the phenotypic evolutionary rate changes [16, 17]. However, ancestral state reconstruction is problematic for any phenotype with imperfect heritability: identical genotypes can then have different phenotypic values, implying an infinitely high rate of phenotypic evolution between them which is not biologically meaningful. Other difficulties arise if the phylogeny is imperfectly reconstructed or the phenotype inaccurately measured, which is always a possibility. Consequently, ancestral state reconstruction does not always provide reliable results, for example when applied to phylogeography [18].

When heritability is not complete, a phenotypic measurement can be seen as just one realisation from the phenotypic distribution of a given individual, with this distribution being what evolves on the tree rather than the phenotypic measurement itself. Based on this idea, here we present a novel Bayesian statistical method which takes as input a phylogenetic tree and discrete tip phenotype measurements, and identifies the branches

on which the phenotype distribution has changed. The tree is therefore divided into 69
monophyletic and paraphyletic groups that have unique distributions over the phenotype 70
space. We also perform Bayesian hypothesis testing [19] to assess whether there is evidence 71
for different parts of the tree having distinct phenotype distributions. We build a stochastic 72
model in which changepoints occur on a phylogenetic tree [20], each of which affects the 73
distribution of observed phenotype for the descendent leaves. Careful parametrisation 74
enables the use of a fixed-dimension Monte-Carlo Markov Chain (MCMC) algorithm [21] 75
to sample from the posterior distribution of the model parameters, and we reserve reversible 76
jumps [22] to compare the model with a model without any changepoint. In the following 77
sections we present our model, inference procedure and the results of simulation studies to 78
measure the sensitivity and specificity of our method. Finally we present the application 79
of our method to two real datasets in HIV evasion and bacterial ecology. 80

Model and Methods

81

Description of the model

82

We consider that changepoints happen as a Poisson process with rate λ on the branches of the input tree. For a phenotype with K categories, we model each changepoint event as a new probability mass function $\mathbf{q} = (q_1, \dots, q_K)$ which specifies the probability of having each of the K phenotypes for the individuals affected by the changepoint. Figure 1 illustrates the model for $K = 2$. The observed phenotype of each individual is shown on the tips of the tree which are coloured as black and red. Changepoints have happened on three branches which divided the tree into four sections (white, blue, green and yellow). All individuals in the same section have the same distribution \mathbf{q} over the phenotype space.

83

84

85

86

87

88

89

90

Let N and B denote the number of tips and branches in the tree, respectively (if the tree is bifurcating then $B = 2N - 2$). We define $\mathbf{b} = (b_1, \dots, b_B)$ as a binary vector with B elements which represent the branches of the tree. If branch i holds at least one changepoint, then $b_i = 1$ else $b_i = 0$. Let m denote the number of sections of the tree divided according to \mathbf{b} (Figure 1), the likelihood of the observed phenotypes of the individuals D is given by:

91

92

93

94

95

$$p(D|\mathbf{q}_1, \dots, \mathbf{q}_m, \mathbf{b}) = \prod_{j=1}^K q_{1j}^{x_{1j}} \cdots \prod_{j=1}^K q_{mj}^{x_{mj}} \quad (1)$$

where $\mathbf{q}_i = (q_{i1}, \dots, q_{iK})$ and q_{ij} gives the probability that an individual in section i expresses phenotype j , so that $\sum_{j=1}^K q_{ij} = 1$ for $i = 1, \dots, m$. We also define $\mathbf{x}_i = (x_{i1}, \dots, x_{iK})$ where x_{ij} is the number of observed individuals in section i which have

96

97

98

expressed phenotype j , so that $\sum_{i=1}^m \sum_{j=1}^K x_{ij} = N$.

99

The prior probabilities of branch i of length l_i having no or at least one changepoint are respectively equal to $\Pr(b_i = 0|\lambda) = e^{-\lambda l_i}$ and $\Pr(b_i = 1|\lambda) = 1 - e^{-\lambda l_i}$, so that:

100

101

$$\Pr(\mathbf{b}|\lambda) = \prod_{i=1}^B (e^{-\lambda l_i})^{1-b_i} (1 - e^{-\lambda l_i})^{b_i} \quad (2)$$

We consider a flat Dirichlet prior for all \mathbf{q}_i such that $p(\mathbf{q}_i) = \Gamma(K)$, and an exponential prior on λ with parameter $1/T$ where $T = \sum_{i=1}^B l_i$ is the sum of the branch lengths of the tree. This implies a parsimonious prior expectation of one for the number of changepoints on the tree.

102

103

104

105

We are now in a position to describe the posterior distribution of the model parameters $\mathbf{q}_1, \dots, \mathbf{q}_m, \mathbf{b}$ and λ :

106

107

$$\begin{aligned} p(\mathbf{q}_1, \dots, \mathbf{q}_m, \mathbf{b}, \lambda | D) &= p(D | \mathbf{q}_1, \dots, \mathbf{q}_m, \mathbf{b}, \lambda) p(\mathbf{q}_1, \dots, \mathbf{q}_m, \mathbf{b}, \lambda) / p(D) \\ &\propto p(D | \mathbf{q}_1, \dots, \mathbf{q}_m, \mathbf{b}) p(\mathbf{q}_1) \dots p(\mathbf{q}_m) p(\mathbf{b} | \lambda) p(\lambda) \\ &\propto (\Gamma(K))^m \prod_{i=1}^m \prod_{j=1}^K q_{ij}^{x_{ij}} \prod_{s=1}^B (e^{-\lambda l_s})^{1-b_s} (1 - e^{-\lambda l_s})^{b_s} T e^{-T\lambda} \end{aligned} \quad (3)$$

The dimensionality of the model parameters changes with \mathbf{b} . If \mathbf{b} divides the tree into two sections then there are four parameters $(\mathbf{q}_1, \mathbf{q}_2, \mathbf{b}, \lambda)$ in the model whereas if \mathbf{b} divides the tree into three sections then there are five parameters $(\mathbf{q}_1, \mathbf{q}_2, \mathbf{q}_3, \mathbf{b}, \lambda)$ in the model. This could potentially be addressed using reversible jumps [22]. Instead we marginalise all the

108

109

110

111

\mathbf{q}_i which results in a fixed dimension model. The marginal posterior density for \mathbf{b} and λ is 112
given by: 113

$$\begin{aligned} p(\mathbf{b}, \lambda | D) &= \int_{\mathbf{q}_1} \cdots \int_{\mathbf{q}_m} p(D | \mathbf{q}_1, \dots, \mathbf{q}_m, \mathbf{b}) p(\mathbf{q}_1) \cdots p(\mathbf{q}_m) d\mathbf{q}_1 \cdots d\mathbf{q}_m p(\mathbf{b} | \lambda) p(\lambda) / p(D) \\ &\propto (\Gamma(K))^m \prod_{i=1}^m \prod_{j=1}^K \int_0^1 q_{ij}^{x_{ij}} dq_{ij} T e^{-T\lambda} \prod_{s=1}^B (e^{-\lambda l_s})^{1-b_s} (1 - e^{-\lambda l_s})^{b_s} \\ &\propto (\Gamma(K))^m \prod_{i=1}^m \frac{\prod_{j=1}^K \Gamma(x_{ij} + 1)}{\Gamma(K + \sum_{j=1}^K x_{ij})} T e^{-T\lambda} \prod_{s=1}^B (e^{-\lambda l_s})^{1-b_s} (1 - e^{-\lambda l_s})^{b_s} \end{aligned} \quad (4)$$

Inference 114

We use a MCMC [21] to sample from the posterior distribution of \mathbf{b} and λ . We use a 115
symmetric proposal for \mathbf{b} where the proposed value \mathbf{b}^* is the same as \mathbf{b} except for one 116
randomly chosen branch i for which $b_i^* = 1 - b_i$. Therefore if the randomly chosen branch i 117
holds a changepoint in \mathbf{b} , it does not hold a changepoint in \mathbf{b}^* and vice versa. To update λ 118
we propose from a normal density with mean equal to the current value of λ and variance 119
equal to 0.1, i.e. $\lambda^* | \lambda \sim \mathcal{N}(\lambda, 0.1)$. When the proposed λ^* is lower than zero, the move is 120
rejected and the chain stays at λ . The calculation of the Metropolis-Hastings acceptance 121
ratios are given in the supplementary material. 122

Model selection 123

We want to assess whether there is any evidence for differential distribution of phenotype 124
on different parts of the tree. We compare our model (indexed 1) against the null model 125

(indexed 0) of no changepoints on the tree, which is equivalent to $\lambda = 0$, by calculating
the Bayes factor [19] for the two models. To do this we use reversible jump moves [22]
to sample from the joint distribution $p((j, \theta_j)|D)$ where j is the index of the model and
 θ_j is the parameters of model j . For a move from null to alternative (0 to 1) model, to
match dimensions we generate two random variables u and \mathbf{v} and map them such that
 $(\lambda^*, \mathbf{b}^*) = (u, \mathbf{v})$. In addition we set the proposal distribution for u and \mathbf{v} , $q(u, \mathbf{v})$ in model
0 to be the same as the prior distribution on λ and \mathbf{b} in model 1. Thus for a proposed
move from model 0 to 1 we have:

$$q(u, \mathbf{v}) = q(u)q(\mathbf{v}|u) = Te^{-Tu} \prod_{i=1}^B (e^{-u l_i})^{1-v_i} (1 - e^{-u l_i})^{v_i} \quad (5)$$

The probability of acceptance of this move is given by:

$$\begin{aligned} h((0) \rightarrow (1, (\lambda^*, \mathbf{b}^*))) &= 1 \wedge \frac{p(1, (\lambda^*, \mathbf{b}^*)|D)p(1 \rightarrow 0)}{p(0|D)p(0 \rightarrow 1)q((u, \mathbf{v})|0)} \left| \frac{\partial(\lambda^*, \mathbf{b}^*)}{\partial(u, \mathbf{v})} \right| \\ &= 1 \wedge \frac{p(1, (u, \mathbf{v})|D)p(1 \rightarrow 0)}{p(0|D)p(0 \rightarrow 1)q((u, \mathbf{v})|0)} \times 1 \\ &= 1 \wedge \frac{p(D|(u, \mathbf{v}), 1)p((u, \mathbf{v})|1)p(1)p(1 \rightarrow 0)}{p(D|0)p(0)p(0 \rightarrow 1)q((u, \mathbf{v})|0)} \\ &= 1 \wedge \frac{p(D|(u, \mathbf{v}), 1)p(1 \rightarrow 0)}{p(D|0)p(0 \rightarrow 1)} \end{aligned} \quad (6)$$

A move from model 1 with parameters (λ, \mathbf{b}) to model 0 is made deterministically and is
accepted with probability:

$$h((1, (\lambda, \mathbf{b})) \rightarrow (0)) = 1 \wedge \frac{p(D|0)p(0 \rightarrow 1)}{p(D|(\lambda, \mathbf{b}), 1)p(1 \rightarrow 0)} \quad (7)$$

We set $p(1 \rightarrow 0) = 0.05$ and $p(0 \rightarrow 1) = 0.5$ and we assume the prior probabilities of the two models are equal $p(0) = p(1) = 0.5$.

Simulation studies

To investigate the performance of our method, we performed two simulation studies each of which involved repetition over many simulated datasets. In all of these simulations for simplicity we used a binary phenotype and sampled from the posterior distribution of the model parameters using 10^7 iterations of our MCMC algorithm. All of these simulations were implemented for a single genealogy simulated using the coalescent model [23] with 1000 leaves shown in Figure S1. First we tested how the number of individuals affected by a changepoint and the magnitude of the change in phenotype distribution affects the statistical power to detect a changepoint. Secondly we tested the model selection procedure and the relationship between the posterior expectation of number of changepoints against the true numbers of changepoints. Thirdly we quantified the effect of threshold on the point estimate of \mathbf{b} .

Results

151

Simulation study of statistical power

152

This simulation study was designed to assess the power of the method to detect
 changepoints on the branches of the tree. The power depends on two factors: the magnitude
 of the change in the distribution over the phenotype categories which we refer to as p and the
 number of individuals affected by the changepoint which we refer to as n . The probability
 of each phenotype is 0.5 before the changepoint, and after the changepoint the probability
 of one phenotype increases by p whereas the probability of the other phenotype decreases
 by p . Changepoints with small p are difficult to detect as they result in small changes
 to the observed pattern of distribution of phenotype that are likely to happen by chance
 alone. Changepoints with small n are also difficult to distinguish as lack of data makes
 the inference more uncertain. We expect that changepoints with large p and large n to be
 easier to detect.

163

The space of $n \times p$ was divided into a grid where $n = (10, 30, 60, 130, 330, 500)$ and $p =$
 $(0.1, 0.2, 0.3, 0.4, 0.5)$. For each node of the grid (p_i, n_j) an appropriate branch of the tree
 shown in Figure S1 was chosen to hold a changepoint, with the remaining branches being
 left free of changepoints. For each node of the grid we simulated 50 datasets each with a
 single changepoint. Figure 2 shows for each node of the grid the mean marginal posterior
 probability of having a changepoint for the branch with the changepoint. A changepoint
 that causes large changes to the distribution of the phenotype categories and affects a large
 number of individuals is inferred with a high posterior probability. Changepoints that cause
 small changes in the distribution or affect few individuals or both result in small posterior
 probability of having a changepoint.

173

Simulation study of model and parameter inference

174

This simulation study was designed to assess our model selection procedure, the effect of 175
number of changepoints on the inference and the effect of cutoff threshold on the point 176
estimate of \mathbf{b} . We simulated 100 datasets for each case of 0, 1, \dots , 10 changing branches 177
in the tree. The distribution over the phenotypes was uniformly sampled in each case. For 178
each simulated dataset the Bayes factor of our model against null model was estimated 179
(Figure 3A). For the 100 datasets with no changepoint on the tree, all the estimated Bayes 180
factors indicated no significant evidence against the null model (no changepoint on the 181
tree) for any of datasets. Changepoints that result in small changes in the distribution or 182
affect small number of individuals will not be detected. Therefore for some of datasets with 183
a single changing branch there is no significant evidence against the null model, but for 184
some there is strong evidence against the null model. As the number of changing branches 185
on the tree increases, the number of datasets with significant evidence for the alternative 186
model increases. Overall, our method is conservative and should not result in significant 187
evidence for the existence of changepoints unless there is substantial data to support it. 188

Next, we used the simulations to gauge the relationship between the true number of 189
simulated changing branches and its posterior expectation, estimated using Bayesian model 190
averaging [24]. Figure 3B illustrates the results. In the absence of any changepoint, the 191
mean of posterior expectation of number of changing branches is always close to zero. When 192
there are changing branches on the tree, the posterior expectation is downward biased 193
compared to the real value. This is expected as our method cannot detect a changepoint 194
that results in small changes in the distribution or affects few individuals or both. As a 195
result our method is conservative in estimating the number of changepoints on the tree. 196

In addition we used the simulation results to assess the effect of a cutoff threshold on the point estimate of \mathbf{b} . For each of the datasets we inferred a point estimate for \mathbf{b} by applying a threshold to the consensus representation of \mathbf{b} (marginal posterior probability of having a changepoint for each branch of the tree). The threshold was changed from 0 to 1 with increments of 0.01. For each threshold value, the false positive rate and the true positive rate across all of our 1100 simulations was calculated. Figure 3C shows the true positive rate as a function of the false positive rate. This so-called ROC curve has a high area under the curve of 0.891, indicative of good performance of the algorithm [25]. The choice of the cutoff threshold is a trade off between minimising the number of incorrectly inferred changepoints and maximising the number of correctly inferred changepoints. This choice depends on the application and the weight given to sensitivity and specificity in the application.

Detecting HIV escape mutations from cytotoxic T-lymphocytes

Human leukocyte antigen (HLA) type I genes encode proteins that are present on the surface of almost all human cells. When a cell is infected with a virus, the viral protein is cleaved and small segments of it called epitopes are presented on the cell surface by the HLA encoded proteins. These proteins have a certain amount of affinity and thus in people with the same HLA allele, the same epitope will be recognised and presented on the cell surface. Cytotoxic T lymphocytes (CTLs) are part of the adaptive immune response and recognise these epitopes before destroying the infected cell. A mutation in one of these epitopes can result in no or weak binding of the peptide to the HLA encoded protein or result in lack of recognition by the T cell receptor. Such mutations lead to the virus escaping the immune response of the host. As these mutations can have a fitness cost

on transmission to a host with different HLA repertoire, they may revert back to the wild 220
type [26]. Thus the escape mutations on the virus genome are correlated with the host's 221
HLA alleles. 222

However to detect these associations one has to account for the possible geographical 223
structuring that could be present in the data. For instance different HCV genotypes are 224
endemic in different parts of the world and HLA allele profiles are also distinct in different 225
populations across the world. When sampling is across different countries or ethnic groups, 226
it is possible that HLA alleles will be associated with specific clusters of the virus simply 227
because of geographical structuring. Several methods have been suggested to account for 228
the non random distribution of HLA alleles on the tips of the phylogenetic tree [27, 28, 29]. 229
We propose that using our algorithm, one can determine if host HLA alleles are randomly 230
distributed on the tips of the virus phylogenetic tree or whether there are clades where 231
the distributions are distinct from each other. The result can then be used to perform 232
stratified association studies conditioned on the clades with distinct HLA distribution. 233

We used previously published data [30] on a cohort of 261 South Africans to detect 234
HLA-driven evolution of HIV. In this study whole genome viral sequences were aligned 235
and then divided into ten fragments of 1000 nucleotides overlapping by 50 nucleotides. 236
Each partition was then used to produce a maximum likelihood phylogenetic tree. The 237
HLA alleles of the patients were also typed. We used the ten phylogenetic trees from this 238
dataset and the HLA information of the patients as the inputs of our algorithm, considering 239
the presence and absence of each HLA type separately. This resulted in 1197 runs of our 240
software. Figure S2 shows the histogram of the Bayes factors estimated by each run. Only 241
the HLA allele B57 and the tree of the first region of the HIV genome had a Bayes factor 242
conclusively rejecting the null model of no association. Figure 4 shows the distribution of 243

the B57 HLA allele on the tips of the first virus phylogeny. There is a clade of twelve viral individuals where ten of the hosts have the B57 allele, whereas across the rest of the tree there are only seven other hosts with B57 HLA alleles. This clear non random distribution of the HLA B57 could be due to transmission of the virus between closely related people. However we do not detect the same association between the other nine trees from the rest of the genome and HLA B57. An alternative explanation may be that HLA B57 has a significant effect on the evolution of the first 1000 nucleotide of the virus, since HLA B57 is associated with slow progression to disease following HIV infection [31, 32].

Inferring host range within a lineage of *Salmonella enterica*

Salmonella enterica is a bacterial pathogen made of multiple lineages with different host ranges [33, 34, 35]. Many lineages can infect a wide range of animals, whereas some are mostly found in specific hosts and yet others have become restricted to a single host type, for example the Typhi and Paratyphi A lineages which evolved in convergence towards infecting only humans [36]. The Typhimurium DT104 lineage has been responsible for a global multidrug resistant epidemic since the 1990s in both humans and farm animals [37, 38, 39]. Typhimurium DT104 can infect both animals and humans, but it is unclear if there are sublineages within DT104 that infect one host type more than the other, and to what extent the epidemics in animals and humans are associated. Traditional molecular typing techniques do not provide enough genetic resolution to answer this question. A recent study sequenced the whole genomes of 142 human strains and 120 animal strains isolated in Scotland between 1990 and 2011 [40]. A maximum-likelihood tree was computed based on the non-recombinant core genome using RAxML [41] and here we applied our algorithm to this tree, using animal versus human source as the phenotype.

The null model of random distribution of hosts around the tree was decisively rejected 267
in favour of the changepoint model, with the reversible jump MCMC never exploring the 268
null model after initial burnin. The posterior mean number of changing branches was 269
9.7, with 95% credibility interval ranging from 5 to 16. Changes in the host range were 270
especially evident on four branches (Figure 5), corresponding to posterior probabilities of 271
99%, 95%, 90% and 72%, with two further branches with probability 54%, one with 39% 272
and all others below 20%. Amongst the four branches with highest support, the oldest 273
corresponds to an increase in the frequency of infection of animals for a large clade of 274
265 isolates within DT104. The other three branches all occurred within this clade, and 275
correspond to three separate further increase in the frequency of infection of animals for 276
three subclades containing 12, 15 and 59 isolates, respectively. These results confirm and 277
refine the original conclusions of the study in which the data was presented [40], that the 278
epidemic of DT104 in Scotland was not homogenous in humans and animals. Specifically, a 279
sublineage increasingly became restricted to infecting only animals and not humans, which 280
could be the result of either adaptation or niche segregation. 281

Discussion

282

This study is based on the concept of phenotype distribution, which is the distribution 283
of phenotypes that a given genotype may express depending on environmental factors, as 284
a result of phenotypic plasticity [2, 3]. We presented a model in which the phenotype 285
distribution is allowed to change along the branches of a phylogenetic tree, and an efficient 286
Bayesian method to perform inference under this model. Given phenotype observations 287
for the leaves of a phylogeny, we showed that our method can be used to detect branches 288
on which the phenotype distribution changed significantly. Consequently, a phylogeny can 289
be demarcated into lineages with distinct phenotype distributions. 290

There are many ways in which our approach could be extended, for example to be applicable 291
to continuous rather than categorical phenotype measurements, or to allow the evolution of 292
the phenotype distribution to be more progressive, for example by making this distribution 293
after a changepoint correlated with, rather than independent from, the distribution before 294
the changepoint. We did not attempt to model the potential for error in either the 295
input phylogeny or input phenotype measurements. Uncertainty about the tree could be 296
accounted for by applying our method to a sample of trees from the posterior distribution of 297
the trees that are produced by Bayesian phylogenetic software such as MrBayes and BEAST 298
[42, 43]. However, we expect that a little inaccuracy in the tree would not drastically affect 299
the result of our method, and likewise for the phenotype measurement, because the results 300
depend on phenotype distributions which are themselves stochastic. This is unlike methods 301
that consider changes in the phenotype itself, such as ancestral state reconstructions [15], 302
for which a mistake in a single phenotype measurement implies an additional evolutionary 303
event for the phenotype. When considering phenotypes with imperfect heritability [1], 304
we argue that modelling the evolution of the phenotype distribution is more biologically 305

relevant than modelling the evolution of the phenotype measurement.

306

There are many research areas in which the method we proposed could be useful, and
we presented two examples in HIV immunology and bacterial ecology. For example, our
approach could help provide a definition of microbial species. Detecting incipient speciation
requires to distinguish between ecologically distinct populations in the same community
[44, 45, 46]. In this case the phenotype would be ecological or pathogenicity measurements,
and the aim is to determine if different phylogenetic clades have distinct distributions
over the measurable ecological quantities [47, 48]. Another potential area of application is
genome wide association studies (GWAS) in organisms that reproduce clonally. Population
structure is a confounding effect in GWAS [49] and this is especially important for clonal
organisms [50]. One way to account for this population structure would be to use our
method to find the clades on the phylogenetic tree where the phenotype of interest is
uniquely distributed and perform GWAS stratified by those clusters.

307

308

309

310

311

312

313

314

315

316

317

318

Acknowledgements

319

This research was made possible by a James Martin fellowship awarded to M. A. Ansari. X. 320
 Didelot received funding from the Biotechnology and Biological Sciences Research Council 321
 (BB/L023458/1) and the National Institute for Health Research (HPRU-2012-10080). The 322
 authors would like to thank Remi Bardenet, Daniel Falush, Philip Maybank and Gil 323
 McVean for their insightful discussions. 324

References

- [1] Visscher PM, Hill WG, Wray NR (2008) Heritability in the genomics era concepts and misconceptions. *Nat Rev Genet* 9:255–266.
- [2] DeWitt TJ, Sih A, Wilson DS (1998) Cost and limits of phenotypic plasticity. *Trends Ecol Evol* 13:77–81.
- [3] Agrawal AA (2001) Phenotypic plasticity in the interactions and evolution of species. *Science* 294:321–326.
- [4] Pritchard JK, Stephens M, Donnelly P (2000) Inference of population structure using multilocus genotype data. *Genetics* 155:945–59.
- [5] Lawson DJ, Hellenthal G, Myers S, Falush D (2012) Inference of population structure using dense haplotype data. *PLoS Genet* 8:e1002453.
- [6] Yang Z, Rannala B (2012) Molecular phylogenetics: principles and practice. *Nat Rev Genet* 13:303–14.
- [7] Didelot X, Falush D (2007) Inference of bacterial microevolution using multilocus sequence data. *Genetics* 175:1251–66.
- [8] Didelot X, Lawson D, Darling A, Falush D (2010) Inference of homologous recombination in bacteria using whole-genome sequences. *Genetics* 186:1435–49.
- [9] Maddison WP (1997) Gene trees in species trees. *Syst Biol* 46:523–536.
- [10] Hillis DM, Huelsenbeck JP (1992) Signal, noise, and reliability in molecular phylogenetic analyses. *J Hered* 83:189–195.

- [11] Blomberg SP, Garland T, Ives AR (2003) Testing for phylogenetic signal in comparative data: behavioral traits are more labile. *Evolution* 57:717–745.
- [12] Garland T, Bennett AF, Rezende EL (2005) Phylogenetic approaches in comparative physiology. *J Exp Biol* 208:3015–35.
- [13] Cunningham CW, Omland KE, Oakley TH (1998) Reconstructing ancestral character states. *Trends Ecol Evol* 13:361–366.
- [14] Pagel M (1999) Inferring the historical patterns of biological evolution. *Nature* 401:877–84.
- [15] Yang Z, Kumar S, Nei M (1995) A new method of inference of ancestral nucleotide and amino acid sequences. *Genetics* 141:1641–1650.
- [16] Revell L (2008) On the Analysis of Evolutionary Change along Single Branches in a Phylogeny. *Am Nat* 172:140–147.
- [17] Revell LJ, Mahler DL, Peres-neto PR, Redelings BD (2011) A New Phylogenetic Method for Identifying Exceptional Phenotypic Diversification. *Evolution* 66:135–146.
- [18] De Maio N, Wu CH, O’Reilly KM, Wilson D (2015) New Routes to Phylogeography: A Bayesian Structured Coalescent Approximation. *PLOS Genet* 11:e1005421.
- [19] Kass RE, Raftery AE (1995) Bayes Factors. *J Am Stat Assoc* 90:773.
- [20] Didelot X, Darling A, Falush D (2009) Inferring genomic flux in bacteria. *Genome Res* 19:306–17.
- [21] Gilks W, Richardson S, Spiegelhalter D (1995) Markov Chain Monte Carlo in Practice. CRC Press.

- [22] Green PJ (1995) Reversible Jump Markov Chain Monte Carlo Computation and Bayesian Model Determination. *Biometrika* 82:711.
- [23] Rosenberg Na, Nordborg M (2002) Genealogical trees, coalescent theory and the analysis of genetic polymorphisms. *Nat Rev Genet* 3:380–90.
- [24] Hoeting JA, Madigan D, Raftery AE, Volinsky CT (1999) Bayesian Model Averaging : Tutorial. *Stat Sci* :382–401.
- [25] Bradley AP (1997) The use of the area under the ROC curve in the evaluation of machine learning algorithms. *Pattern Recognit* 30:1145–1159.
- [26] Leslie AJ, Pfafferott KJ, Chetty P, Draenert R, Addo MM, et al. (2004) HIV evolution: CTL escape mutation and reversion after transmission. *Nat Med* 10:282–9.
- [27] Bhattacharya T, Daniels M, Heckerman D, Foley B, Frahm N, et al. (2007) Founder effects in the assessment of HIV polymorphisms and HLA allele associations. *Science* 315:1583–6.
- [28] Carlson JM, Brumme ZL, Rousseau CM, Brumme CJ, Matthews P, et al. (2008) Phylogenetic dependency networks: inferring patterns of CTL escape and codon covariation in HIV-1 Gag. *PLoS Comput Biol* 4:e1000225.
- [29] Carlson JM, Listgarten J, Pfeifer N, Tan V, Kadie C, et al. (2012) Widespread impact of HLA restriction on immune control and escape pathways of HIV-1. *J Virol* 86:5230–43.
- [30] Rousseau CM, Daniels MG, Carlson JM, Kadie C, Crawford H, et al. (2008) HLA Class I-Driven Evolution of Human Immunodeficiency Virus Type 1 Subtype C Proteome: Immune Escape and Viral Load. *J Virol* 82:6434–6446.

- [31] Altfield M, Addo MM, Rosenberg ES, Hecht FM, Lee PK, et al. (2003) Influence of HLA-B57 on clinical presentation and viral control during acute HIV-1 infection. *AIDS* 17:2581–2591.
- [32] Miura T, Brockman MA, Schneidewind A, Lobritz M, Pereyra F, et al. (2009) HLA-B57/B*5801 Human Immunodeficiency Virus Type 1 Elite Controllers Select for Rare Gag Variants Associated with Reduced Viral Replication Capacity and Strong Cytotoxic T-Lymphocyte Recognition. *J Virol* 83:2743–2755.
- [33] Uzzau S, Brown DJ, Wallis T, Rubino S, Leori G, et al. (2000) Host adapted serotypes of *Salmonella enterica*. *Epidemiol Infect* 125:229–55.
- [34] Didelot X, Bowden R, Street T, Golubchik T, Spencer C, et al. (2011) Recombination and population structure in *Salmonella enterica*. *PLoS Genet* 7:e1002191.
- [35] Achtman M, Wain J, Weill FX, Nair S, Zhou Z, et al. (2012) Multilocus sequence typing as a replacement for serotyping in *Salmonella enterica*. *PLoS Pathog* 8:e1002776.
- [36] Didelot X, Achtman M, Parkhill J, Thomson NR, Falush D (2007) A bimodal pattern of relatedness between the *Salmonella* Paratyphi A and Typhi genomes: convergence or divergence by homologous recombination? *Genome Res* 17:61–8.
- [37] Glynn MKA, Bopp CH, Dewitt W, Dabney P, Mokhtar M, et al. (1998) Typhimurium Dt104 Infections in the United States. *N Engl J Med* 338:1333–1338.
- [38] Mølbak K, Baggesen D, Møller Aarestrup F, Ebbesen J, Engberg J, et al. (1999) An outbreak of multidrug-resistant, quinolone-resistant *Salmonella Enterica* serotype Typhimurium DT104. *N Engl J Med* :1420–1425.
- [39] Threlfall EJ (2000) Epidemic *Salmonella typhimurium* DT 104 a truly international. *J Antimicrob Chemother* 46:7–10.

- [40] Mather AE, Reid SWJ, Maskell DJ, Parkhill J, Fookes MC, et al. (2013) Distinguishable epidemics of multidrug-resistant Salmonella Typhimurium DT104 in different hosts. *Science* 341:1514–1517.
- [41] Stamatakis A (2006) RAxML-VI-HPC: maximum likelihood-based phylogenetic analyses with thousands of taxa and mixed models. *Bioinformatics* 22:2688–90.
- [42] Huelsenbeck JP, Ronquist F (2001) MRBAYES: Bayesian inference of phylogenetic trees. *Bioinformatics* 17:754–5.
- [43] Drummond AJ, Suchard Ma, Xie D, Rambaut A (2012) Bayesian phylogenetics with BEAUti and the BEAST 1.7. *Mol Biol Evol* 29:1969–73.
- [44] Ferris MJ, Köhl M, Wieland A, Ward DM (2003) Cyanobacterial ecotypes in different optical microenvironments of a 68 degrees C hot spring mat community revealed by 16S-23S rRNA internal transcribed spacer region variation. *Appl Environ Microbiol* 69:2893–8.
- [45] Sikorski J, Nevo E (2005) Adaptation and incipient sympatric speciation of *Bacillus simplex* under microclimatic contrast at "Evolution Canyons" I and II, Israel. *Proc Natl Acad Sci U S A* 102:15924–9.
- [46] Johnson ZI, Zinser ER, Coe A, McNulty NP, Woodward EMS, et al. (2006) Niche partitioning among *Prochlorococcus* ecotypes along ocean-scale environmental gradients. *Science* (80-) 311:1737–40.
- [47] Achtman M, Wagner M (2008) Microbial diversity and the genetic nature of microbial species. *Nat Rev Microbiol* 6:431–40.
- [48] Fraser C, Alm EJ, Polz MF, Spratt BG, Hanage WP (2009) The bacterial species challenge: making sense of genetic and ecological diversity. *Science* (80-) 323:741–6.

- [49] Marchini J, Cardon LR, Phillips MS, Donnelly P (2004) The effects of human 434
population structure on large genetic association studies. Nat Genet 36:512–7. 435
- [50] Earle SG, Wu Ch, Charlesworth J, Stoesser N, Gordon NC, et al. (2016) Controlling 436
for population structure in bacterial association studies. Nat Microbiol :in press. 437

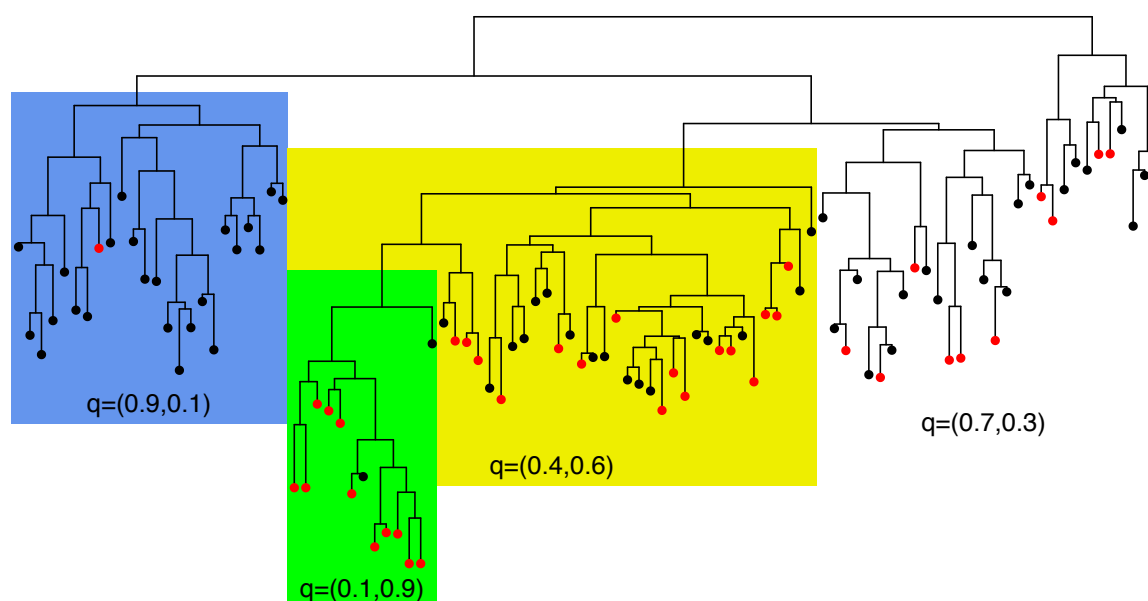


Figure 1. Illustration of the model. Changepoints occurred on three branches, which divided the tree into four sections (white, blue, green and yellow), each of which has different probabilities of the first (black) and second (red) phenotypes.

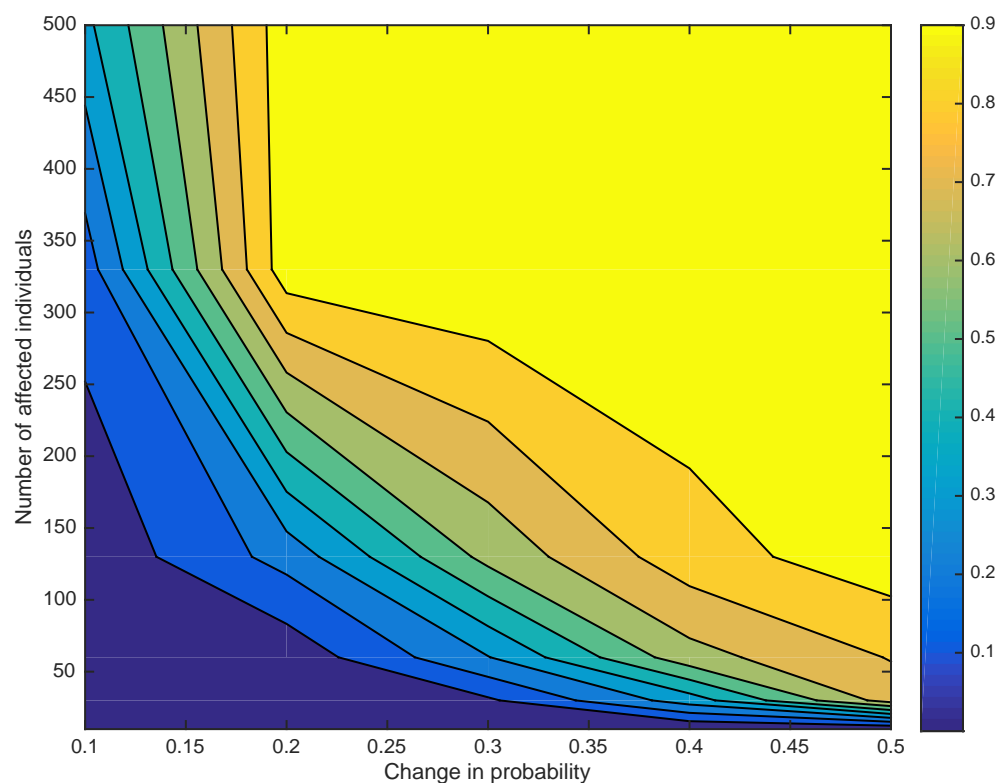


Figure 2. Effect of number of strains and change in distribution. Contour plot of the mean posterior probability of having a changepoint as a function of number n of affected individuals and the magnitude p of the change in distribution. The space of $n \times p$ was divided into a grid where $n = (10, 30, 60, 130, 330, 500)$ and $p = (0.1, 0.2, 0.3, 0.4, 0.5)$.

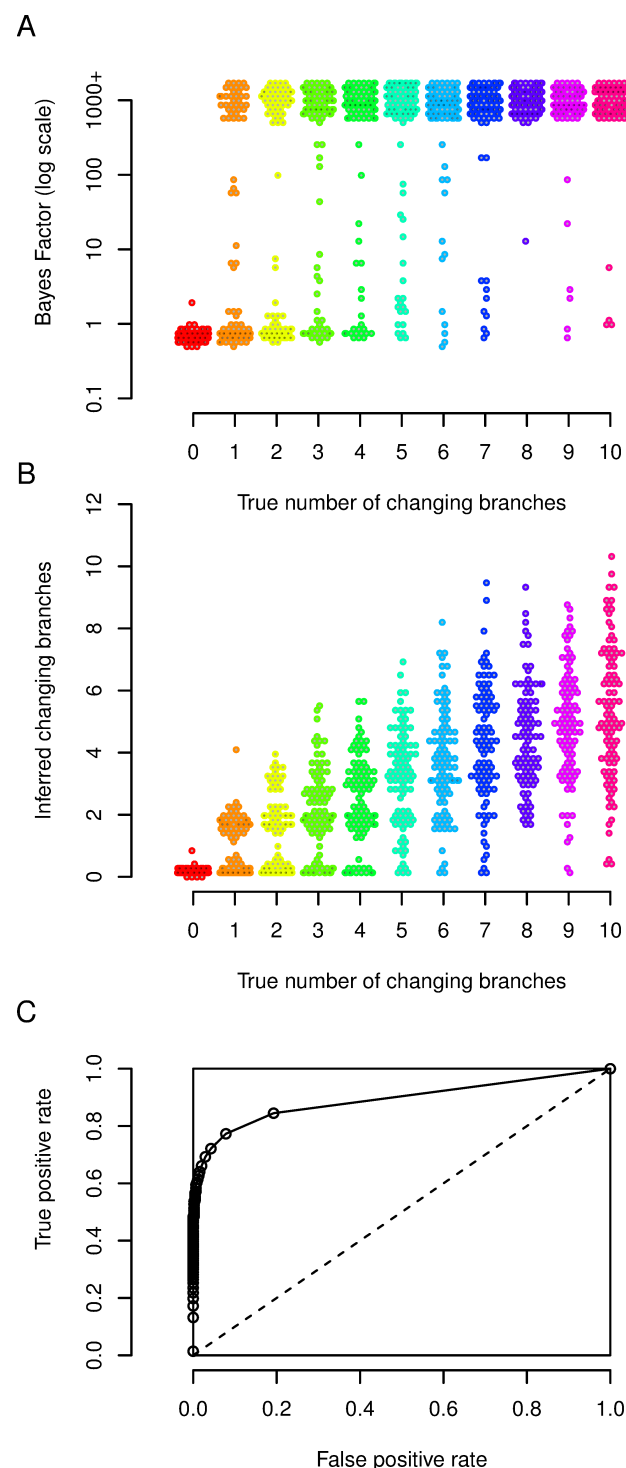


Figure 3. Simulation study of model and parameter inference. (A) Bayes factor values for the changepoint model versus the null model, as a function of the number of changing branches used in the simulation. (B) Distribution of posterior mean number of changing branches as a function of the true number of simulated changing branches. (C) ROC curve: true positive rate as a function of the false positive rate.

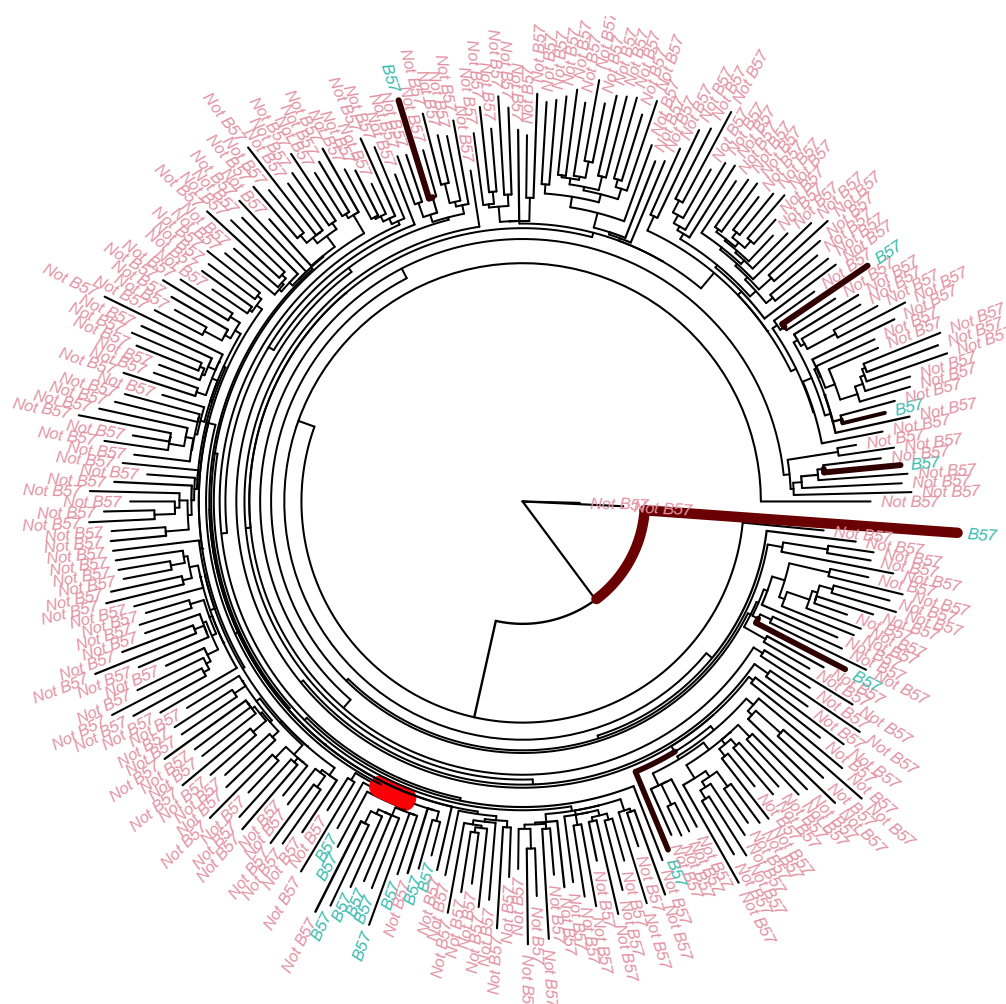


Figure 4. Application to HIV immunology. Phylogenetic tree of 261 HIV infected individuals from the first 1000 nucleotides with the tips coloured according to presence and absence of HLA B57 in the host. The thickness and colour of the branches are proportional to the posterior probability of having a changepoint.

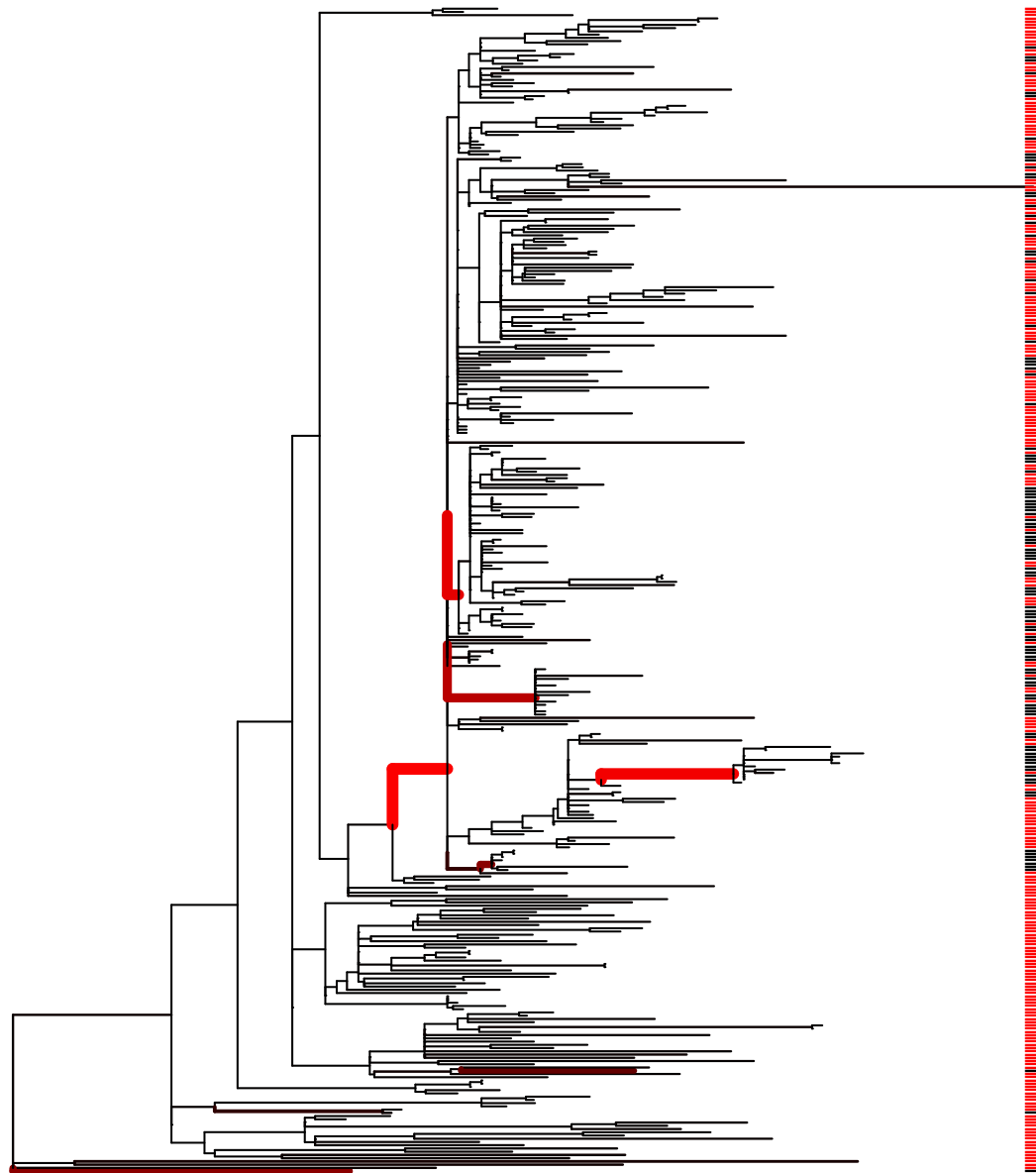


Figure 5. Application to *Salmonella* ecology. Maximum-likelihood phylogenetic tree from a previous study of Typhimurium DT104 [40], with the color on the right indicating the isolates came from either human (red) or animal (black) sources. The results of our algorithm are shown by the thickness and redness of the branches, which are both proportional to the posterior probability of host range change on the given branch.